

适用于 CH₄ 泄漏检测的全光光声光谱装置

杨腾飞^{1,2}, 康文运³, 朱文越¹, 刘 强^{1*}, 钱仙妹¹, 梅海平¹, 陈 杰¹, 杨 韬^{1,2}, 郑健捷¹

- 中国科学院合肥物质科学研究院安徽光学精密机械研究所 激光与物质相互作用全国重点实验室, 安徽合肥 230031;
- 中国科学技术大学研究生院科学岛分院, 安徽合肥 230026;
- 北京跟踪与通信技术研究所, 北京 100094)

摘要: 光声光谱技术是一种高灵敏的光学检测技术,已成功应用于各种痕量气体检测场合。针对工业上 CH₄ 气体泄漏的快速安全检测问题,研制了一套基于 H 形光声池和 Fabry-Perot 干涉式光纤麦克风的全光光声光谱装置。采用有限元分析方法对悬臂梁的振动特性进行了仿真分析,并优化了悬臂梁的结构参数,使其共振频率和光声池的共振频率相匹配,实现了对光声信号的双共振增强。同时利用平面镜使光声吸收池的投射光再次入射进入吸收池,进一步增强了光声信号。装置使用 Q 点稳定强度解调程序对干涉信号进行解调,解决了光纤麦克风在测试过程中的 Q 点随温度漂移的问题,确保了光纤麦克风长期工作时的稳定性。该光声测量装置采用 1 653 nm 波长 DFB 激光器作为激发光源,利用 Q 点稳定强度解调方法,结合波长调制-二次谐波检测技术、声学共振放大技术实现了对 CH₄ 气体的全光、高灵敏度检测。实验结果表明,全光光声光谱装置的共振频率为 1 594 Hz,在共振频率处 CH₄ 气体的检测极限为 7.47 ppm (1 ppm=1×10⁻⁶)。根据 Allan 方差结果,在 142 s 的平均时间下,全光光声光谱装置测量 CH₄ 气体的检测极限为 0.23 ppm。

关键词: 光纤传感; CH₄ 气体探测; 全光光声光谱; 光纤麦克风; 悬臂梁

中图分类号: TP212 **文献标志码:** A **DOI:** 10.3788/IRLA20240314

0 引言

甲烷 (CH₄) 气体检测在大气污染监测^[1]、畜牧养殖监测^[2]、煤矿安全^[3] 和医疗诊断^[4] 等领域具有重要作用,同时 CH₄ 气体的高灵敏快速检测对于工业事故预警和减少损失具有重要意义^[5]。CH₄ 气体检测方法包括电化学法^[6]、可调谐二极管吸收光谱法 (TDLAS)^[7]、燃烧催化法^[8]、非色散红外法 (NDIR)^[9] 和光声光谱法 (PAS)^[10] 等。电化学法测量 CH₄ 气体具有高灵敏度特性,但是其需要频繁的校准。燃烧催化法具有快速的时间响应,但是在低氧情况下会产生误差^[11]。随着激光技术以及信号探测及处理技术的高速发展,光声光谱法以其响应速度快、灵敏度高和零背景^[12] 等特性,在痕量气体检测领域受到了越来越广

泛的关注。

传统光声光谱技术采用电容式麦克风作为声信号传感器,电容式麦克风的电学特性限制了其在电磁干扰 (EMI)^[13]、高温和爆炸^[14] 等恶劣环境中的应用。除了传统的光声光谱技术外,近年来也发展了许多新型的光声光谱技术,例如石英音叉增强光声光谱技术 (QEPAS)^[15]、悬臂增强光声光谱技术 (CEPAS) 以及全光光声光谱技术^[16] 等。石英音叉具有灵敏度高、体积小和耐腐蚀性的优点。石英音叉产生的电信号较弱,限制了在高电磁干扰环境中的应用^[12]。悬臂增强光声光谱技术采用了迈克尔逊干涉结构,这会使系统变得复杂。全光光声光谱技术采用全光学原理探测光声信号,具有抗电磁干扰的优点,可应用于高电磁

收稿日期:2024-07-29; 修订日期:2024-08-30

基金项目:中国科学院合肥物质科学研究院院长基金 (E33DEG12)

作者简介:杨腾飞,男,硕士生,主要从事激光光谱、光纤传感和光声光谱等方面的研究。

导师简介:朱文越,男,研究员,博士,主要从事激光大气传输和大气光学特性等方面的研究。

通讯作者:刘强,男,副研究员,博士,主要从事大气光学特性和激光大气探测技术等方面的研究。

干扰环境^[17-18]。全光光声光谱技术根据光纤麦克风设计原理分为基于光纤布拉格光栅 (FBG) 的全光 PAS 和基于干涉仪的全光 PAS 等。基于 FBG 的全光 PAS 会受光谱边带的影响, 这降低了 FBG 声学传感器的灵敏度^[12]。基于 Fabry-Perot 干涉式的光纤麦克风采用光学干涉原理, 具有传感区域集中、环境适应性强、易小型化和灵敏度高等优点^[19], 吸引了更多研究人员的关注。2011 年, WANG 等人首次使用聚醚砜酮 (PPESK) 薄膜制成了 Fabry-Perot 干涉式光纤麦克风^[20], 并利用基于此麦克风开发的全光光声光谱仪开展了乙炔 (C₂H₂) 气体测量研究, 检测极限为 1.56 ppb (1 ppb=1×10⁻⁹)。2018 年, ZHANG 等人利用石墨烯薄膜研制了一款光纤麦克风, 结合微型谐振腔对光声信号进行放大, 并将光纤麦克风的共振频率与微谐振管的谐振频率进行了匹配, 在 138 mW 的激光功率和 1 s 的积分时间下检测 C₂H₂ 气体, 实现了 25 ppb 的检测极限^[21]。为了进一步提高全光光声光谱系统的灵敏度, 研究人员开发了不同的解调技术。2018 年, CHEN 等报道了一种基于锁相的白光干涉 (White light interference, WLI) 解调全光 PAS 技术^[22]。该技术采用宽带光源对光纤麦克风进行调制, 并使用高速白光干涉仪对光纤麦克风的腔长进行解调, 光声信号通过解调 F-P 腔长度的高频分量来恢复。该方法降低了光损耗, 提高了系统的环境温度适应能力, 具有灵敏度高、稳定性好、动态范围宽等优点。为了满足狭小环境下光纤麦克风的应用需求, 2022 年, WU 等报道了一种小型化高灵敏度 Fabry-Perot 光纤麦克风^[23], 该麦克风体积仅有 102 mm³, 在 2500 Hz 频率处的声压灵敏度为 1506 nm/Pa。由此可见, 基于 F-P 干涉仪的全光学 PAS 技术有灵敏度高, 抗电磁干扰能力强和易于小型化等优点, 具有较好的应用前景。文中为进一步提高检测极限, 自主研发了一款外征 Fabry-Perot 光纤麦克风, 并将其与共振型光声吸收池和波长调制技术相结合, 建立了一套 1653 nm 波段的 CH₄ 气体全光光声光谱测量装置, 通过 Allan 方差分析, 测量装置在 142 s 平均时间下可实现 0.23 ppm (1ppm=1×10⁻⁶) 的检测极限。

1 检测原理

1.1 全光光声光谱原理

全光光声光谱测量装置主要包括光声信号产生

和光声信号检测两部分, 这两部分均采用光学原理, 从而具有更强的抗电磁干扰能力和易燃易爆环境下的适应能力。光束通过光声池, 光声信号的幅值为:

$$S_{PA} = C_{cell} \alpha P_0 C \quad (1)$$

式中: C_{cell} 为光声池的池常数, 包括了光声吸收池的共振放大能力和声探测器对弱信号的探测能力; α 为气体吸收系数; P_0 为激光器的光功率; C 为池中气体浓度。

光声信号检测由基于 Fabry-Perot 干涉仪原理的光纤麦克风完成。光纤麦克风的光纤端面 and 振动端面反射的两束光之间的相位差 $\Delta\varphi$ 为:

$$\Delta\varphi = \frac{2\pi}{\lambda} \Delta l = \frac{4\pi n d}{\lambda} \quad (2)$$

式中: λ 为探测光源的波长; Δl 为两个端面的光程差; n 为 F-P 腔中介质的折射率; d 为 F-P 腔的腔长。若探测光源波长为 I_0 , 则经过光纤端面后干涉信号光强为^[24]:

$$I_R = \left(R_1 + \xi R_2 - 2\sqrt{R_1 \xi R_2} \cos \frac{4\pi n d}{\lambda} \right) I_0 \quad (3)$$

式中: R_1 为光纤端面的反射率; R_2 为振动端面的反射率; ξ 为干涉系统的耦合损耗系数。若光纤中的模场半径为 ω_0 , 则 ξ 的大小为^[25]:

$$\xi = \frac{4 \left[1 + \left(\frac{2\lambda d}{\pi n \omega_0^2} \right)^2 \right]}{\left[2 + \left(\frac{2\lambda d}{\pi n \omega_0^2} \right)^2 \right]^2} \quad (4)$$

1.2 吸收谱线选取

基于公式 (1), 光声信号的强度与气体吸收系数成正比, 选取合适的吸收线有利于提高 PAS 系统的检测灵敏度。该测量装置采用中心波长为 1654 nm 的 DFB 激光器 (NEL, NLK1 U5 FAAA) 作为激发光源, 其输出波长范围为 1653~1655 nm。图 1 给出了该波段范围内主要大气分子的吸收光谱, 分子吸收光谱的参数来自 HITRAN 2020 数据库^[26], CO₂, CH₄ 和 H₂O 分子浓度分别为 500 ppm, 10 ppm 和 1%, 根据模拟计算结果, 文中选择 1653.7 nm 附近相对独立的 CH₄ 吸收线进行测量, 图中灰色部分为激光器的实际扫描范围。

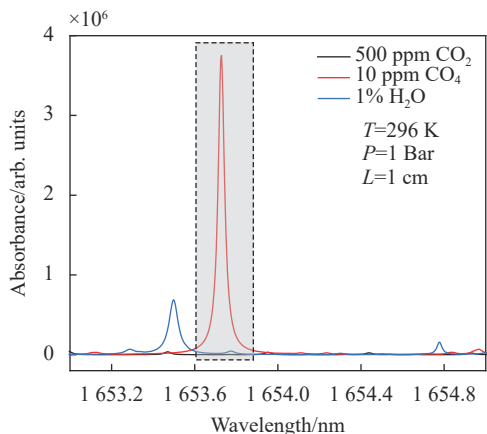


图 1 CO₂, CH₄ 和 H₂O 的吸收谱

Fig.1 Absorption spectrum of CO₂, CH₄ and H₂O

2 实验装置

如图 2 所示, 实验装置采用 1653 nm 波长的激光

器 DFB1(NEL, NLK1 U5 FAAA) 产生激光光源, 利用函数发生器(南京盛普, SP-F20)生成的 2 Hz 三角波作激光器输出波长的扫描信号, 并用锁相放大器(SRS, SR830)输出的正弦信号(约 800 Hz)作为调制信号。调制后的激光入射进入 H 形光声吸收池并激发光声信号, 光声吸收池的另一侧安装反射镜来增大光声池内气体的有效光功率^[27], 进而增强光声信号。用光阑对反射回来的光进行隔离, 以防止反射光重新耦合进入激光器造成激光器的损坏。自主研发的光纤麦克风安装在光声吸收池的中部, 用于检测光声信号。光纤麦克风的探测光源为 DFB2(NEL, NLK1B5E-AAA), 其输出波长为 1310 nm。DFB2 产生的激光经过环形器进入光纤麦克风。光纤麦克风产生干涉信号经光电探测器(Thorlabs, PDA10CF-EC)转化成电信号。电信号经过锁相放大器的解调和放大, 由信号采集卡(NI, USB-6003)采集并由计算机接收。

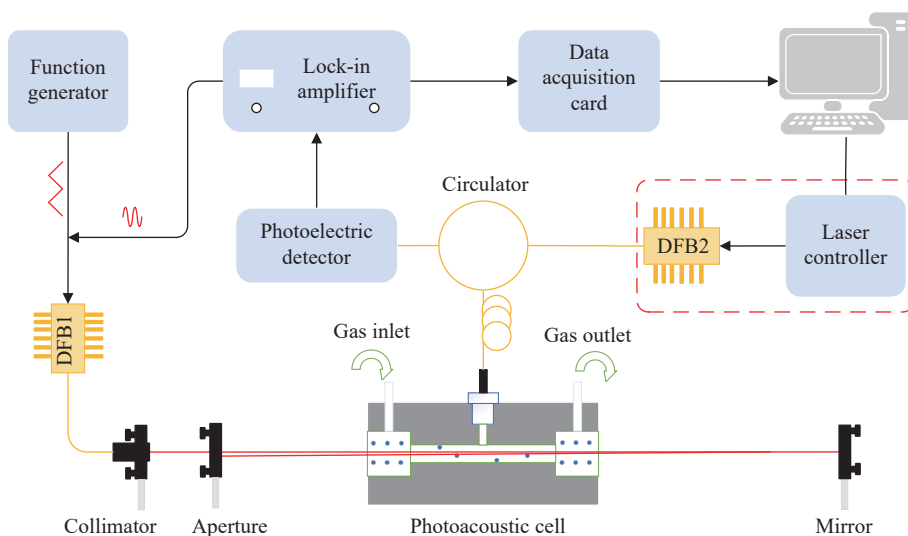


图 2 实验装置图

Fig.2 Diagram of the experimental device

3 实验结果与讨论

3.1 光纤麦克风的仿真与结构设计

文中基于 Fabry-Perot 干涉仪原理设计了一款悬臂梁光纤麦克风。首先用 COMSOL 软件仿真分析了悬臂梁的振动特征, 如图 3 所示。图 3(a) 给出了悬臂梁的结构及第一共振模态的能量分布, 悬臂梁的自由端形变量最大, 能量最高, 悬臂梁的固定端形变量最

小, 能量最低, 右下为悬臂梁芯片实物图。为使悬臂梁共振频率与光声池共振频率相匹配, 实现共振增强, 对悬臂梁的共振频率与其尺寸的依赖关系进行了仿真, 结果如图 3(b) 所示, 悬臂梁的共振频率会随着长度的增长和厚度的增加而降低。由于悬臂梁芯片太厚会降低悬臂梁的振动幅度, 进而降低信号检测的灵敏度, 太薄在振动过程中容易被折断, 文中采用的悬臂梁厚度为 7 μm。为匹配共振频率在 1600 Hz 附

近的光声池,悬臂梁的厚度、宽度和长度分别为 7 μm 、1.2 mm 和 2.35 mm。

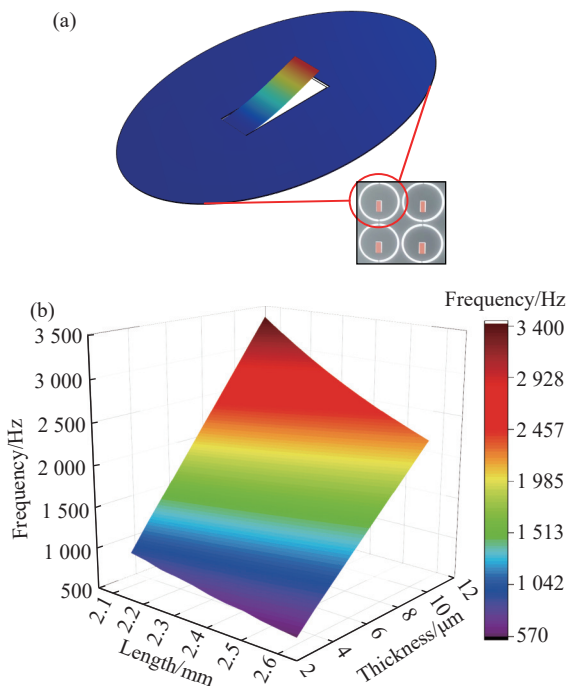


图 3 (a) 悬臂梁仿真图 (右下为悬臂梁实物图); (b) 第一共振频率与悬臂梁的长度和厚度之间的关系

Fig.3 (a) Simulation chart of cantilever beam (The lower right is the physical diagram of the cantilever beam); (b) The relationship between the first-order resonance frequency and the thickness and length of the cantilever

光纤麦克风探头的内部结构和实物如图 4 所示,主要包括 FC 光纤头、不锈钢夹持器、悬臂梁芯片三

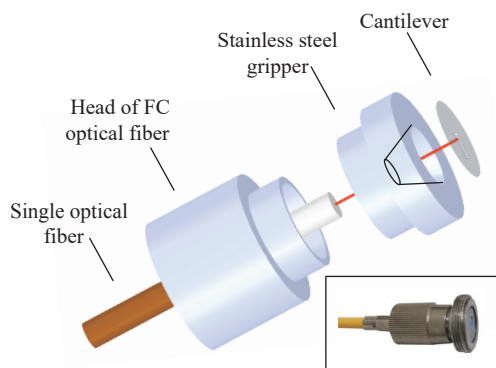


图 4 悬臂梁麦克风内部结构图 (右下图为悬臂梁麦克风实物图)

Fig.4 Diagram of the internal structure of the cantilever microphone (The lower right is the physical diagram of the cantilever microphone)

部分。不锈钢夹持器与悬臂梁芯片之间为圆台形的空腔,其顶部半径为 1.5 mm,底部半径为 3.0 mm,整个探头的体积约为 1600 mm^3 。FC 光纤头的光纤端面和悬臂梁之间形成 F-P 腔,其中二者之间的距离控制在 0.21 mm 左右,该长度即为 F-P 腔的长度。

3.2 光纤麦克风稳定性控制

在实验中,光纤麦克风的腔长会随着环境温度的改变而产生漂移,从而影响干涉信号的稳定性。根据公式 (2),干涉信号的相位差变化 $\Delta\phi$ 与 d 成正比并且与 λ 成反比, d 的改变可通过调控激光器的输出波长 λ 来弥补。文中在此原理的基础上编写了 Q 点稳定的强度解调程序。该程序通过实时控制激光器的波长输出来降低环境温度对光纤麦克风的影响,以确保检测装置始终工作在线性区域^[28]。图 5(a) 灰色部分为实现该解调程序的实验装置。该装置由 DFB2、激

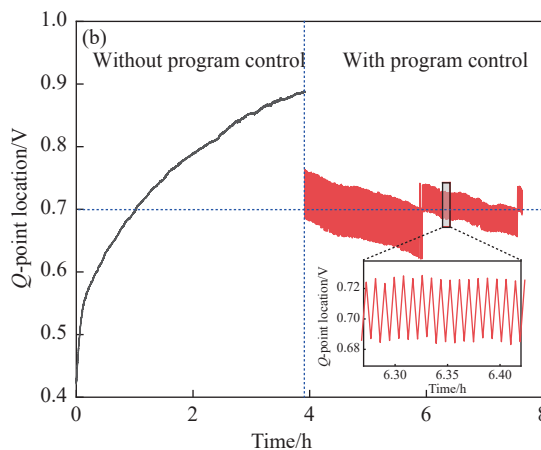
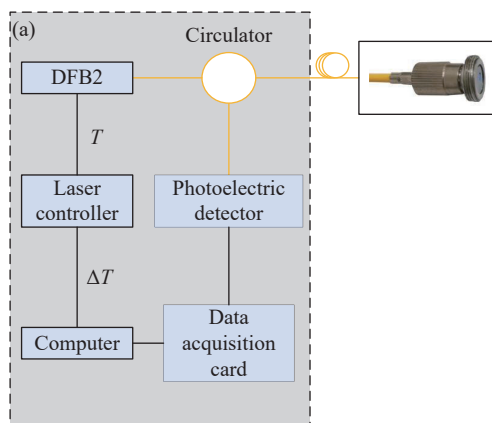


图 5 (a) 程序调控实验装置图; (b) Q 点稳定程序调控前后对比图

Fig.5 (a) Diagram of the experimental device for program control; (b) Comparison diagram before and after Q -point stabilization program control

光控制器、计算机、采集卡、光电探测器和环形器组成。激光控制器通过控制温度参数改变激光器输出的光波长。激光器产生的光源经过光纤麦克风产生干涉信号。干涉信号经光电探测器实现模拟信号到电信号的转换。电信号由采集卡采集并输入计算机。在计算机中实时监测 Q 点的位置, 如果 Q 点不在线性区域的中点^[28], 程序会向激光控制器反馈一个温度变化量 ΔT , 从而改变激光器的波长输出, 以此达到控制 Q 点稳定的目的。为验证设计的解调程序的控制效果, 实验中通过对麦克风在没有控制程序与有控制程序的条件下采集到的 Q 点位置进行了对比。如图 5(b) 所示, 给定 Q 点中心位置为 0.7 V, 结果显示没有程序控制的 Q 点在 4 h 内会发生较大的漂移, 这会造成干涉信号失真, 影响后续干涉信号的解调。有控制程序时, Q 点的位置被成功控制在 0.7 V 附近。该解调程序有效保证了光纤麦克风长时间工作的稳定性。

3.3 全光 PAS 装置性能测试

该实验装置中所采用的悬臂梁光纤麦克风和光声池都会对光声信号共振放大, 为获得更佳的光声信号, 对整个 PAS 装置的频率响应进行了测试。实验中将 500 ppm 的 CH_4 气体通入光声池, 调节激励光源的调制频率, 得到不同调制频率下的光声信号幅值, 结果如图 6 所示。通过拟合得到装置的共振频率为 1 594 Hz, 激光器波长调制频率为其二分之一, 即 797 Hz (二次谐波解调)。后续实验均按此参数设置激励光源的调制频率。

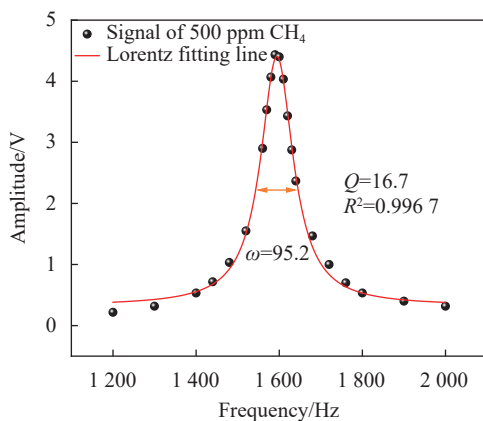


图 6 光声测量装置的频率响应

Fig.6 Frequency response of a photoacoustic measurement device

为了研究光声测量装置的线性响应特性, 实验中使用多成分气体混合系统 (EnviroNics, SERIES 4000) 配制了 20、50、100、200、500 ppm 的 CH_4 气体, 并测量了相应的波长调制-二次谐波信号 (2f-WMS), 如图 7(a) 所示。图 7(b) 为不同 CH_4 气体浓度下 2f-WMS 幅值的拟合函数, 拟合函数的斜率表示 CH_4 气体检测装置的线性响应度, 截距表示装置的背景噪声水平。拟合的相关系数 R^2 为 0.999 8, 表明光声测量装置与 CH_4 气体浓度之间呈良好的线性关系, 线性响应度为 0.013 39 V/ppm。

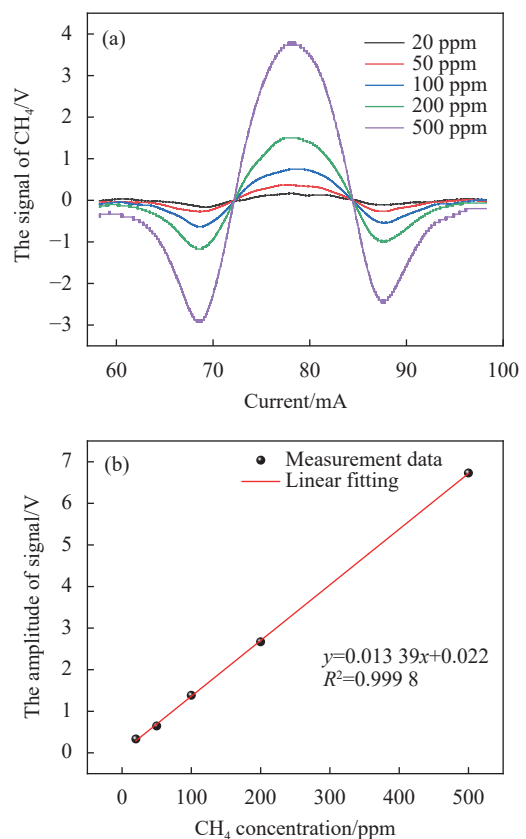


图 7 (a) 光声装置测试不同浓度 CH_4 的 2f-WMS 信号; (b) 光声装置对 CH_4 浓度的响应

Fig.7 (a) The photoacoustic measurement device tests the 2f-WMS signal at different concentrations of CH_4 ; (b) Response of photoacoustic device to the CH_4 concentration

检测极限和稳定性是评估 PAS 系统非常重要的指标。该实验在光声池中通入纯 N_2 用以测量整个检测装置的噪声水平, 采样时间间隔为 1 s。1 000 s 内装置的噪声水平如图 8(a) 所示, 一倍标准差 (1σ) 为 0.10 V, 根据 0.013 39 V/ppm 的线性响应度, 计算出测

量装置的检测极限为 7.47 ppm。通过 Allan 方差分析,对装置的检测灵敏度和稳定性进行评估。图 8(b)显示了 Allan 方差结果,图中添加了基线以显示 Allan 方差结果的趋势,它们之间较好的拟合趋势表明:该光声检测装置具有较好的稳定性,并且实验中的主要噪声为高斯噪声^[29]。高斯噪声主要来源于光电探测器的噪声、悬臂梁芯片的振动噪声、激光功率的抖动和激光波长的波动等。因此,可以通过更长的平均时间来提高检测装置的灵敏度。当平均时间为 142 s 时,CH₄ 气体的最低检测极限 (MDL) 为 0.23 ppm。

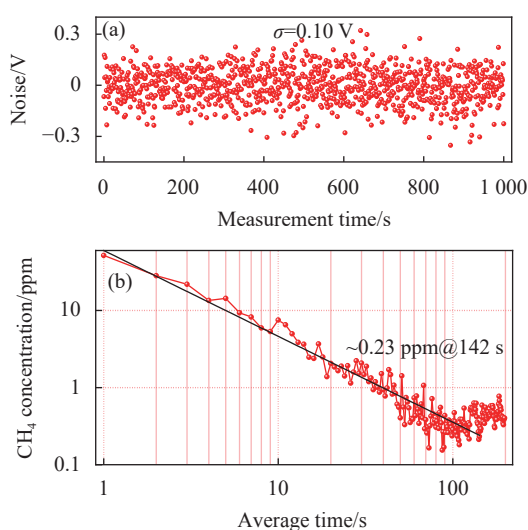


图 8 (a) 1 000 s 内的光声装置背景噪声; (b) Allan 方差分析结果

Fig.8 (a) Background noise of photoacoustic device within 1 000 s; (b) Allan variance results

4 结 论

文中通过对悬臂梁的仿真优化,设计了一款悬臂梁光纤麦克风。采用 Q 点稳定的强度解调技术降低了环境温度对麦克风的干扰,进而确保了光纤麦克风长期工作的稳定性。实验将光纤麦克风与 H 形光声池共振频率相匹配,实现了对光声信号的双共振增强,并搭建了一套高灵敏度全光光声光谱实验装置。该实验装置的声信号的产生与探测均采用光学原理以及光纤结构,实现了 CH₄ 气体的全光、高灵敏度检测。实验装置对 CH₄ 气体的检测极限为 7.47 ppm。根据 Allan 方差结果,在平均时间为 142 s 的条件下,全光光声光谱装置的最小检测极限为 0.23 ppm。该实验中所提出的光声传感装置具有安全性好和结构

简单等特点。目前搭建的光声装置能够满足工业上 CH₄ 气体泄漏的检测水平。该装置目前仅使用平面镜进行了一次反射,后续研究可以结合多通池结构,通过增加气体的吸收光程来获得更高的检测灵敏度,为更高层次的痕量气体探测提供新途径。

参考文献:

- [1] WU Hongpeng, DONG Lei, YIN Xukun, et al. Atmospheric CH₄ measurement near a landfill using an ICL-based QEPAS sensor with V-T relaxation self-calibration [J]. *Sensors and Actuators B: Chemical*, 2019, 297: 126753.
- [2] NEGUSSIE E, LEHTINEN J, MÄNTYSAARI P, et al. Non-invasive individual methane measurement in dairy cows [J]. *Animal*, 2017, 11(5): 890-899.
- [3] CHENG Bo, CHENG Xin, CHEN Junliang, et al. Lightweight monitoring and control system for coal mine safety using REST style [J]. *ISA Transactions*, 2015, 54: 229-239.
- [4] JAHJAH M, REN Wei, STEFAŃSKI P, et al. A compact QCL based methane and nitrous oxide sensor for environmental and medical applications [J]. *Analyst*, 2014, 139(9): 2065-2069.
- [5] GUO Min, CHEN Ke, YANG Beilei, et al. Miniaturized anti-interference cantilever-enhanced fiber-optic photoacoustic methane sensor [J]. *Sensors and Actuators B: Chemical*, 2022, 370: 132446.
- [6] WU Da, LIU Yang, CHEN Wu, et al. The comparative study on the monitoring methods of gas generation in electrochemical treatment process of wastewater [J]. *Guangdong Chemical Industry*, 2018, 7: 139-144. (in Chinese)
- [7] JIANG Jun, ZHAO Mingxin, MA Guoming, et al. TDLAS-based detection of dissolved methane in power transformer oil and field application [J]. *IEEE Sensors Journal*, 2018, 18: 2318-2325.
- [8] CHOUDHARY T V, BANERJEE S, CHOUDHARY V R, et al. Catalysts for combustion of methane and lower alkanes [J]. *Applied Catalysis A: General*, 2002, 234(2): 1-23.
- [9] HODGKINSON J, SMITH R, HO W O, et al. Non-dispersive infra-red (NDIR) measurement of carbon dioxide at 4.2 μm in a compact and optically efficient sensor [J]. *Sensors and Actuators B: Chemical*, 2013, 186: 580-588.
- [10] ZHAO Yandong, FANG Yonghua, LI Yangyu, et al. Design and optimization of Helmholtz-based photoacoustic spectroscopic sensor for multi-gas detection [J]. *Infrared and Laser Engineering*, 2017, 46(6): 0620005. (in Chinese)
- [11] WANG Qiang, WANG Zhen, REN Wei, et al. Wavelength-

- stabilization-based photoacoustic spectroscopy for methane detection [J]. *Measurement Science and Technology*, 2017, 28: 065102.
- [12] YANG Tianhe, CHEN Weigen, WANG Pinyi, et al. A review of all-optical photoacoustic spectroscopy as a gas sensing method [J]. *Applied Spectroscopy Reviews*, 2021, 56(2): 143-170.
- [13] GUAN Liwei, LU Yu, HE Zhijie, et al. Design and development of an intelligent security alarm system based on optical fiber sensing [J]. *Infrared and Laser Engineering*, 2022, 51(8): 20220028. (in Chinese)
- [14] SHAWNA F Gallegos, EDGAR O Aviles-Rosa, MALLORY T DeChant, et al. Explosive odor signature profiling: A review of recent advances in technical analysis and detection [J]. *Forensic Science International*, 2023, 347: 111652.
- [15] KUMAR K, FRANCESCO P, SUN Bo, et al. Highly selective and sensitive detection of volatile organic compounds using long wavelength InAs-based quantum cascade lasers through quartz-enhanced photoacoustic spectroscopy [J]. *Applied Physics Reviews*, 2024, 11(2): 021427.
- [16] ZHAO Xinyu, QI Hongchao, XU Yufu, et al. Fiber-optic photoacoustic gas sensing: a review [J]. *Applied Spectroscopy Reviews*, 2024, 1-29.
- [17] WU Guojie, ZHANG Yongjia, GONG Zhenfeng, et al. A mini-resonant photoacoustic sensor based on a sphere-cylinder coupled acoustic resonator for high-sensitivity trace gas sensing [J]. *Photoacoustics*, 2024, 37: 2213-5979.
- [18] WU Guojie, WU Xue, GONG Zhenfeng, et al. Highly sensitive trace gas detection based on a miniaturized 3D-printed Y-type resonant photoacoustic cell [J]. *Optics Express*, 2023, 31(21): 34213-34223.
- [19] GONG Zhenfeng, WU Guojie, XING Jiawei, et al. Research progress of interferometric all-optical photoacoustic spectroscopy for gas sensing [J]. *Acta Optica Sinica*, 2023, 43(18): 230490. (in Chinese)
- [20] WANG Qiaoyun, WANG Jianwei, LI Liang, et al. An all-optical photoacoustic spectrometer for trace gas detection [J]. *Sensors and Actuator B: Chemical*, 2011, 153: 214-218.
- [21] ZHANG Congzhe, YANG Yuanhong, TAN Yanzhen, et al. All-optical fiber photoacoustic gas sensor with double resonant enhancement [J]. *IEEE Photonics Technology Letters*, 2018, 30(20): 1752-1755.
- [22] CHEN Ke, YU Zhihao, GONG Zhenfeng, et al. Lock-in white-light-interferometry-based all-optical photoacoustic spectrometer [J]. *Optics Letters*, 2018, 43: 5038-5041.
- [23] WU Guojie, LI Haie, YE Hongxin, et al. Ultra-high-sensitivity, miniaturized fabry-perot interferometric fiber-optic microphone for weak acoustic signals detection [J]. *Sensors*, 2022, 22(18): 6948.
- [24] GONG Zhenfeng. Fiber-optic acoustic sensing based trace gas analyzer by using photoacoustic spectroscopy technology[D]. Dalian: Dalian University of Technology, 2018. (in Chinese)
- [25] LI Cheng, GAO Xiangyang, GUO Tingting, et al. Analyzing the applicability of miniature ultra-high sensitivity Fabry-Perot acoustic sensor using a nanothick graphene diaphragm [J]. *Measurement Science and Technology*, 2015, 26(8): 085101.
- [26] GORDON I E, ROTHMAN L S, HARGREAVES R J, et al. The HITRAN2020 molecular spectroscopic database [J]. *Journal of Quantitative Spectroscopy and Radiative Transfer*, 2022, 277: 107949.
- [27] ZHANG Ming, ZHANG Bo, CHEN Ke, et al. Miniaturized multi-pass cell based photoacoustic gas sensor for parts-per-billion level acetylene detection [J]. *Sensors and Actuators A: Physical*, 2020, 308: 112013.
- [28] ZHANG Junping, ZHAO Xinyu, ZHENG Yongqiu, et al. A wide frequency response Fabry-Pérot acoustic sensor based on the self-stabilization system [J]. *IEEE Sensors Journal*, 2023, 23(15): 16922-16929.
- [29] ZHANG Bo, CHEN Ke, CHEN Yewei, et al. High-sensitivity photoacoustic gas detector by employing multi-pass cell and fiber-optic microphone [J]. *Optics Express*, 2020, 28: 6618-6630.

All-optical photoacoustic spectroscopy device for CH₄ leak detection

YANG Tengfei^{1,2}, KANG Wenyun³, ZHU Wenyue¹, LIU Qiang^{1*}, QIAN Xianmei¹, MEI Haiping¹,
CHEN Jie¹, YANG Tao^{1,2}, ZHENG Jianjie¹

(1. State Key Laboratory of Laser Interaction with Matter, Anhui Institute of Optics and Fine Mechanics, HFIPS, Chinese Academy of Sciences, Hefei 230031, China;

2. Science Island Branch of Graduate School, University of Science and Technology of China, Hefei 230026, China;

3. Beijing Institute of Tracking and Telecommunications Technology, Beijing 100094, China)

Abstract:

Objective Methane (CH₄) gas detection plays an important role in many fields, and rapid detection of CH₄ gas is of great significance for early warning of accidents. CH₄ gas detection methods include electrochemical method, tunable diode absorption spectroscopy (TDLAS), combustion catalytic method, non-dispersive infrared method (NDIR), photoacoustic spectroscopy (PAS), etc. Electrochemical measurement of CH₄ gas has high sensitivity properties, but it requires frequent calibration. Combustion catalysis has a fast time response, but produces error in low oxygen. With the rapid development of laser technology and acoustic detection technology, photoacoustic spectroscopy has attracted more and more attention for its fast response, zero background and high sensitivity in trace gas detection. Traditional photoacoustic spectroscopy technology using capacitive microphone as acoustic signal sensor, but the electrical characteristics of the capacitive microphone limits in electromagnetic interference (EMI), high temperature and explosive environmental applications. Fabry-Perot interferometric fiber microphone has the advantages of concentrated sensing area, strong environmental adaptability, easy miniaturization and high sensitivity. In recent years, the all-optical PAS technology based on the Fabry-Perot interferometer has attracted the attention of many researchers. A feasible experimental scheme is proposed for the rapid and safe detection of CH₄ gas leakage in industry by using fiber microphone based Fabry-Perot interferometric principle. Now it is enough to be used in the industrial leak detection of CH₄ gas, which is contributed to achieve methane gas leakage warning and protect workers safe.

Methods Traditional photoacoustic spectroscopy techniques use condenser microphones as photoacoustic signal sensors, but the electrical characteristics of capacitive microphones limit their use in environments such as electromagnetic interference. In this paper, an all-optical photoacoustic spectroscopy device for CH₄ gas leakage detection is proposed. The technology is divided into photoacoustic signal generation module and photoacoustic signal detection module. The photoacoustic signal generation module is as follows. The excitation light source generated by the modulated 1 653 nm DFB laser enters the photoacoustic cell to generate a photoacoustic signal, the photoacoustic signal is received by the optical fiber microphone, and the photoacoustic signal is transformed from the optical signal to the optical signal through the optical fiber microphone; The photoacoustic signal demodulation module is as follows. The light source generated by the 1 310 nm DFB laser enters the Fabry-Perot (F-P) cavity through the circulator to form an interference signal. Then the self-made optical fiber microphone is used for acquisition, and the interference optical signal is demodulated by the intensity demodulation method based on temperature feedback adjustment, and the advantage of this method is to achieve stable control of the interference signal Q point for a long time and quick response. The final signal is amplified by a lock-in amplifier, collected by the signal acquisition card (NI, USB-6003), and input into the computer to realize the detection of

the generated photoacoustic signal.

Results and Discussions The CH₄ gas in the laboratory is tested using the photoacoustic spectroscopy device. The experimental results show that the detection limit of using the optical fiber optic microphone is 7.47 ppm (1 ppm=1×10⁶). According to the Allan variance results, the detection limit of CH₄ gas is 0.23 ppm at an average time of 142 s. Compared with other photoacoustic spectroscopy technologies, the proposed photoacoustic sensing system has the advantages of good stability, fast response speed and simple optical path, and the whole experimental system is simple.

Conclusions A cantilever fiber optic microphone is designed through the simulation and optimization of the cantilever beam. The *Q*-point stabilized intensity demodulation technology reduces the interference of the ambient temperature to the microphone, thereby ensuring the stability of the fiber microphone for long-term operation. In the experiment, the resonance frequency of the optical fiber microphone and the H-shaped photoacoustic cell was matched to realize the double resonance enhancement of the photoacoustic signal, and a set of high-sensitivity all-optical photoacoustic spectroscopy experimental device was built. The acoustic signal generation and detection of the experimental device are based on optical principle and optical fiber structure, which realizes the all-optical and high-sensitivity detection of CH₄ gas. The detection limit of the experimental setup for CH₄ gas was 7.47 ppm. According to the Allan variance results, the minimum detection limit of the all-optical photoacoustic spectroscopy device is 0.23 ppm under the condition of an average time of 142 s. The photoacoustic sensing system proposed in this experiment has the characteristics of good safety and simple structure. At present, the photoacoustic device can meet the detection level of CH₄ gas leakage in the industry.

Key words: optical fiber sensing; CH₄ gas detection; all-optical photoacoustic spectroscopy; fiber-optic microphone; cantilever beam

Funding projects: President Fund of the Hefei Institutes of Physical Science, Chinese Academy of Sciences (E33DEG12)